JOURNAL OF AIRCRAFT
Vol. 37, No. 6, November–December 2000

Validation and Operation of a Wake Vortex/Shear Interaction Model

Z. C. Zheng* and S. H. Lim†
University of South Alabama, Mobile, Alabama 36688-0002

A vortex method model developed previously for studying the mechanisms in vortex/shear-layer interactions has been validated with large-eddy turbulence simulations by Proctor et al. (Proctor, F. H., Hinton, D. A., Han, J., Schowalter, D. G., and Lin, Y. L., "Two Dimensional Wake Vortex Simulations in the Atmosphere: Preliminary Sensitivity Studies," AIAA Paper 97-0056, Jan. 1997) and field measurement data. A shear-detection algorithm used to incorporate meteorological wind data is developed. Operational issues are also explored. The shear-thickness effects and the wind measurement resolution requirement and its sensitivity to the prediction algorithm are discussed. The objective of this work is to develop a computational method that is both accurate enough for the intended purpose and rapid enough to be of use in an operational setting at airports.

Introduction

AIRCRAFT wake vortex behavior has been an important safety consideration in air-traffic management. Unanticipated encounters with wake vortices during terminal flight operations are highly undesirable. A significant effort is underway at the NASA Langley Research Center to develop the aircraft vortex spacing system (AVOSS), which will determine safe operating spacings between arriving and departing aircraft, on the basis of observed/predicted weather state.[1]

Atmospheric wind shear conditions can significantly influence the motion of wake vortices, thus changing the duration that these vortices stay in the AVOSS-defined aircraft approach corridor.[2] According to the NASA 1994 and 1995 field measurement program in Memphis, Tennessee,[3] the descending wake vortices could stall or be deflected at the top of low-level temperature inversions after sunset. These temperature inversions are usually associated with pronounced shear zones.

Proctor et al.'s[1] tests indicated that the mechanisms responsible for the asymmetric deflection (i.e., one vortex in the vortex pair retains higher altitude than the other) in the trailing vortices could be deduced possibly from inviscid interactions between the vortex pair and shear layers. On the basis of that hypothesis, a vortex method model has been developed by Zheng and Baek.[4] In that model, the primary trailing vortex pair is represented by two opposite-sign point vortices. A shear layer is modeled by a layer of vortices with constant circulation. Figure 1 illustrates the initial distributions of vortices for simulating interactions between the wake vortex pair and the shear layer below it. Several examples of the interactions have been shown in Ref. 4. The model simulation results have shown that if a shear layer is placed beneath the vortex pair with the same sign as the left vortex, the right vortex descends less than the left vortex. When the same shear layer is placed above the vortex pair, the right vortex descends more than the left one. This descent altitude difference increases with the shear-layer strength. Those trends are qualitatively in agreement with the prediction of the Navier–Stokes (N–S) simulations by Proctor et al.[1] The physical mechanisms were fully discussed in Ref. 4 and are briefly explained here. When the shear layer (with the same sign vorticity as the left vortex in the vortex pair) is below the vortex pair, the vortex pair approaches the shear layer and deforms the shear layer gradually. Some of the vortices in the shear layer are pushed downward, due to the induced downwash by the vortex pair, and some are lifted and wrapped around the vortex pair when the vortex pair is close to the shear layer. The opposite-sign vortices near the right vortex tend to reduce the vertical motion of the right vortex, similar to the mechanism of vortex rebound near the ground, which is due to the induced opposite-sign secondary vortices from the ground boundary. Therefore, after some time of interactions, the right vortex descends less than the left vortex. If the same shear layer is placed above the vortex pair, the vortices in the shear layer are pulled in between the vortex pair, due to the shape of streamlines around the vortex pair. Because the vortices from the shear layer are in the middle of the vortex pair, they produce the opposite effects and induce upward motion on the left vortex and downward motion on the right vortex and eventually cause the right vortex to descend more than the left vortex.

The current study quantitatively compares the model results with Proctor et al.'s[1] N–S simulations with large-eddy turbulence models, as well as field measurement data.[5] Because the vortex method is much faster than the N–S simulations, this model can be used for real-time vortex modeling on the basis of measured wind-shear profiles. An algorithm used to incorporate meteorological wind data is developed. Operational issues are also explored. The shear thickness effects and the wind measurement resolution requirement and its sensitivity to the prediction algorithm are discussed. The model used in this paper is the least complicated model that can include enough physics to simulate the asymmetric deflection of the vortex pair approaching a strong, concentrated shear. To the authors' knowledge, this paper was the first effort in which such models were implemented for wake vortex prediction and validation. Simpler models were developed[6] by adding one term in a vortex decay equation to model the shear effects. However, those models are usually unable to properly simulate the physics and fail to predict correct vortex deflection trends under concentrated shear environment.

Model Validation

We have compared the model results with Proctor et al.'s[1] large-eddy turbulence model simulations. Two cases of strong shear (3 and 4 m/s shear in Ref. 1) have been chosen for comparison, and the results are shown in Fig. 2. It can be seen that good agreement has been obtained for both cases, with differences at later times possibly caused by effects not included in the model, such as stratification and turbulence in the large-eddy simulations. The right vortex, which has the opposite-sign circulation of the shear layer, shows better agreement in both cases. The reason is that the right vortex, which deflects from the shear zone due to interactions with the shear, is away from the ground boundary, and its trajectory is mostly determined by the

Received 27 December 1999; presented as Paper 2000-0626 at the 38th Aerospace Sciences Meeting, Reno, NV, 11–15 January 2000; revision received 8 May 2000; accepted for publication 8 May 2000.

*Assistant Professor, Mechanical Engineering Department; zzheng@jaguar1.usouthal.edu. Senior Member AIAA.
†Graduate Research Assistant.

shear/vortex interaction. Therefore, the model includes most of the physics for the behavior of the right vortex. On the other hand, the left vortex descends close to the ground and the ground secondary vortices also influence its trajectory, an effect that the current model does not include. However, some overpredictions of the right vortex bounce were noticed. Because the shear–layer vortices are responsible for the bounce in the simulation, the reason is that the decay of the shear-layer vortices is not included in the model. The stronger (than reality) shear vortices cause extra deflection of the right vortex.

To validate the model via field measurement data, the tower fly-by data collected in FAA Idaho Falls (IDF) measurement have been selected for validation.[5] The flight tests utilized B757-200, B727-222, and B767-200 airplanes. Many of the tests produced inconclusive or incomplete data. For difficult measurements such as aircraft wake vortices, which also require simultaneous meteorological measurements, the difficulty level of data interpretation can increase significantly. Three cases, named run 22, run 9, and run 45,[7] are identified to be tested on typical shear-layer effects. The run 22 case (a B727-222 flight test) has a strong, concentrated shear layer with near-neutral stratification. The run 9 case (a B757-200 flight test) has a strong but not so concentrated shear layer with stable stratification. The run 45 case (a B757-200 flight test) has a weak, broad shear layer with stable stratification. The surface wind profiles for these three cases were measured from meteorological measurement and are plotted in Fig. 3. It has been noticed that the existence of a strong, concentrated shear requires special meteorological conditions, such as strong temperature inversions.

The decay histories and vortex behavior near the ground were measured in detail in IDF flight tests. Therefore, the model in Ref. 4, which does not have decay and ground effects, needs to be modified

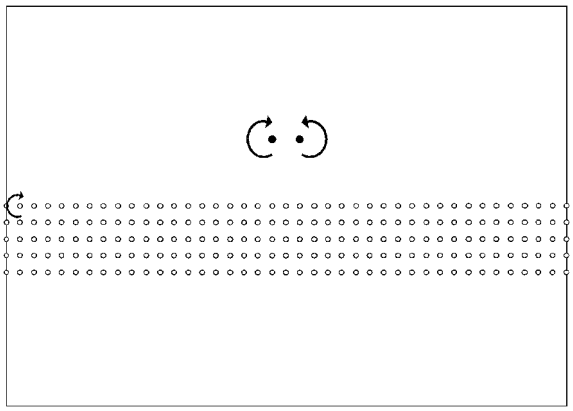

Fig. 1 Initial positions of vortices in the wake vortex/shear interaction model.

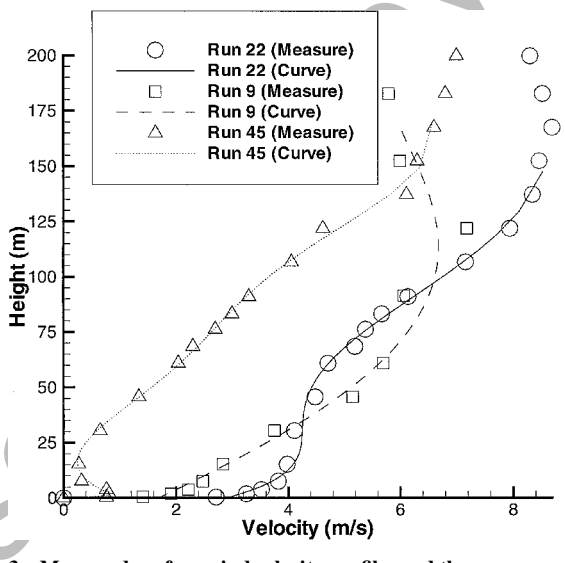

Fig. 3 Measured surface wind velocity profiles and the corresponding fitted curves for the three Idaho Falls flight-test cases.

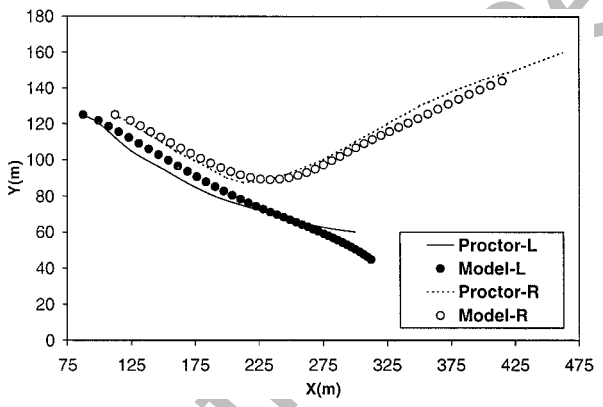

Trajectories of 3 m/s shear case

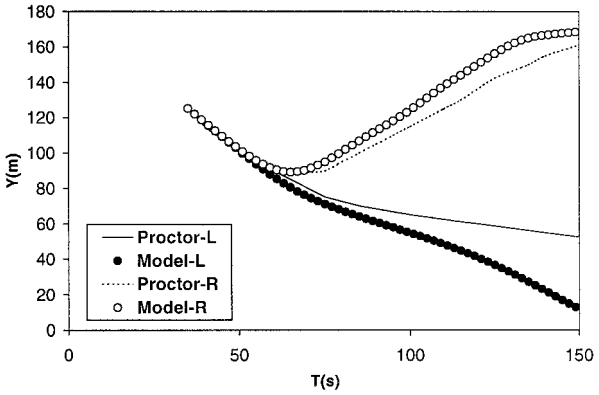

Altitudes vs time of 3 m/s shear case

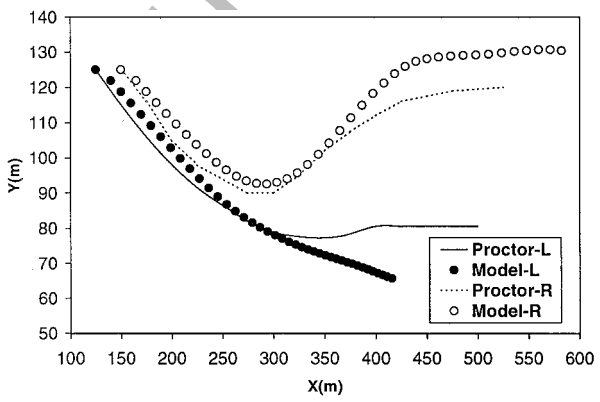

Trajectories of 4 m/s shear case

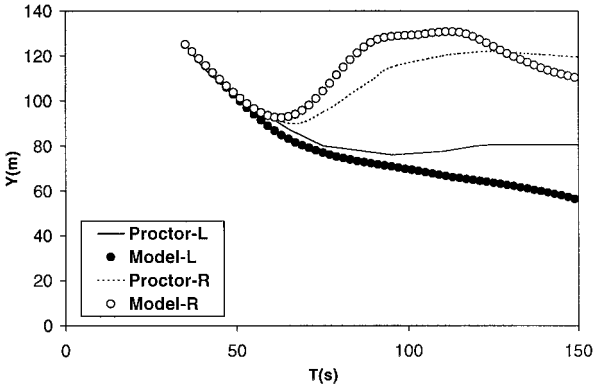

Altitudes vs time of 4 m/s shear case

Fig. 2 Comparison of the model results with Proctor et al.'s[1] results.

to include these effects. Ground effects on vortex transport can be approximated in the model by using image vortices. The wake-induced secondary vortices[8] near the ground are not simulated in the modification. Under the condition that a strong shear layer appears near the ground, the secondary ground vortices are likely to have negligible effects compared with shear effects. The ground then just behaves as a reflection boundary. Therefore, the equation used in the vortex method becomes

$$\frac{d\bar{z}_p}{dt} = -\frac{i}{2L}\sum_{q=1,q\neq p}^{N}\Gamma_q \cot\frac{\pi(z_p - z_q)}{L} + \frac{i}{2L}\sum_{q=1}^{N}\Gamma_q \cot\frac{\pi(z_p - \bar{z}_q)}{L} \quad (1)$$

where $z = x + iy$ and $\bar{z}$ is the complex conjugate of z, with $y = 0$ being the location of the ground boundary, and L is the periodic wavelength in the x direction (lateral direction) for the periodic boundary conditions employed in the x direction.

Greene[9] and more recently Sarpkaya[10] have developed wake vortex decay models that include effects from stratification and atmospheric turbulence. Greene's model also includes a term for the effects of viscous drag, although with minor contribution relative to the other terms.[10] If buoyancy force and viscous drag are ignored, both models give an analytical solution in the exponential function form

$$\Gamma/\Gamma_o = \exp(-kt) \quad (2)$$

where k depends on the atmospheric turbulence intensity, and Γ and Γ_o are the instantaneous and initial circulations of the wake vortices, respectively. In Greene's model, the decay coefficient k is a function of atmospheric turbulent kinetic energy (TKE), whereas in Sarpkaya's model, it is a function of turbulent-eddy dissipation rates and Brunt-Vaisala frequency of stratification. Unfortunately, there were no simultaneous TKE and dissipation rate measurement data in IDF data set for the three test cases. Therefore, in the following validation cases, the values of k are based on the least-squares curve fitting of the measured circulation decay data (of both right and left vortices) for the exponential base function in Eq. (2). The circulation decay histories for the model and the measured data are shown graphically in each of the following cases (later in Figs. 4–6), and the least-squares fitted values of k are listed in Table 1. It should be noted that the negative circulation data in measurement, which are nonphysical and were caused by the loss of signal of vortex tracking, were not accounted for in the least-squares fitting for determining the k values.

The wake vortex decay coefficient, k, is then used in the vortex method Eq. (1) but only for the circulation of the vortex pair.

Table 1 Parameters used for each run provided by ASDA

Parameter	Run 22	Run 9	Run 45
u_1, m/s	3.88	5.76	4.72
u_2, m/s	2.71	1.41	0.23
u_{conv}, m/s	3.88	3.585	2.475
x_o, m	−106.68	−106.68	−106.68
y_o, m	76.2	70	79.26
B_o, m	25.84	30	30
Γ_o, m^2/s	316.9	365	365
H, m	14.2	68.01	122.03
S_{range}, m	0.4–14.6	0.5–68.51	23.73–145.76
Γ_s, %	0.96	2.57	2.15
Δy	0.14	0.325	0.51
k	0.0220	0.0108	0.0150

u_{conv} is the convective speed of the vortex pair; x_o and y_o are the initial positions of the left vortex in the wake vortex pair, respectively; B_o is the initial span of the vortex pair; S_{range} is the altitude range of the shear location; Γ_s is the shear layer circulation in percentage of the initial wake vortex circulation; Δy is the initial vertical direction resolution of the shear layer; and k is the wake vortex decay coefficient nondimensionalized with Γ_o and B_o.

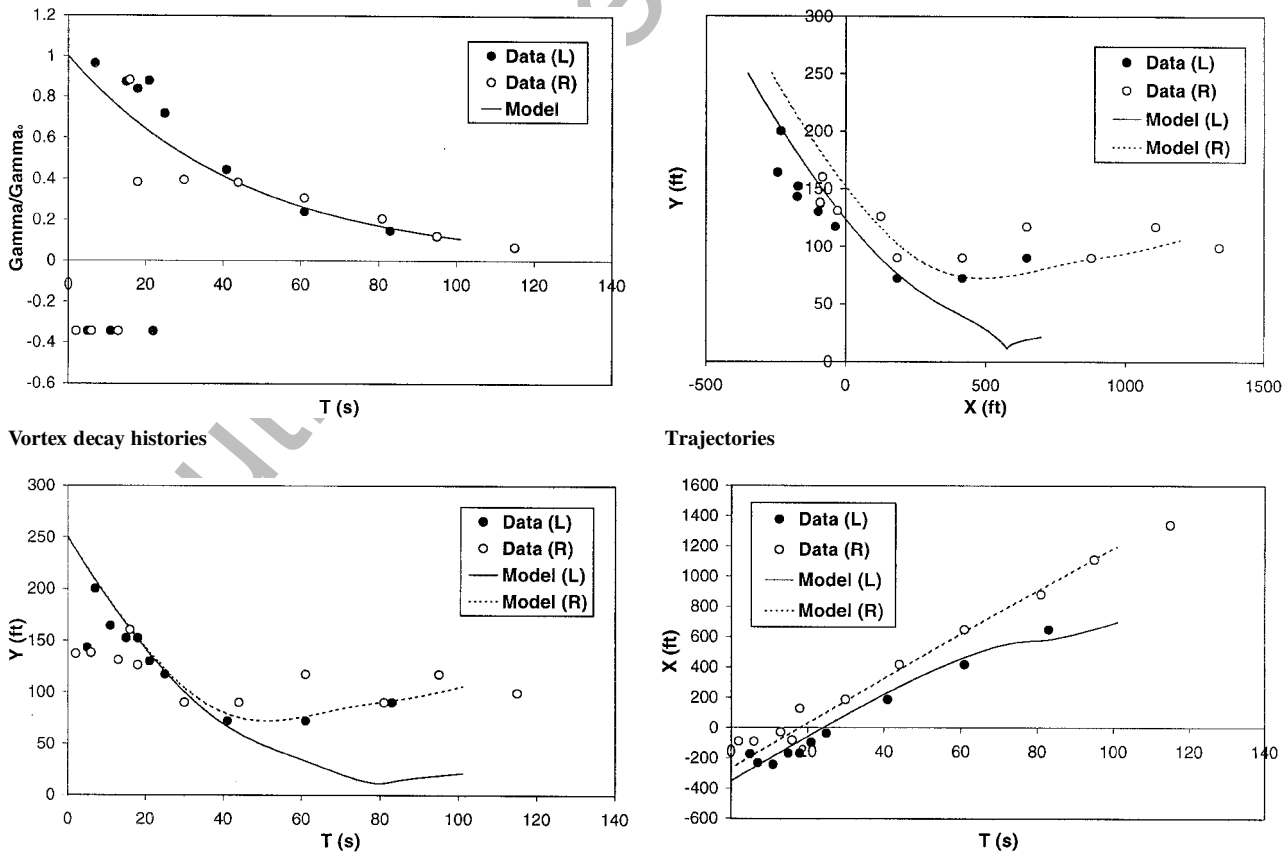

Fig. 4 Comparison of the model results with field-measurement data of the run 22 case.

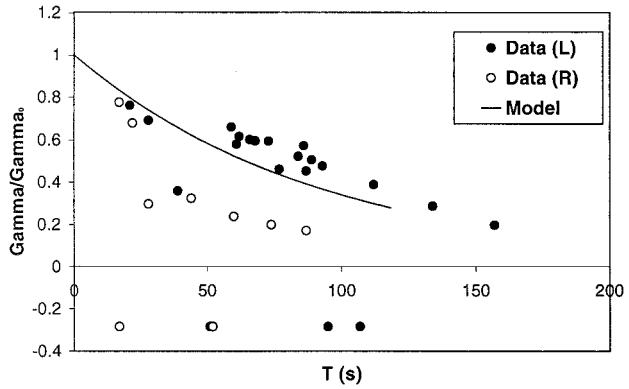

Vortex decay histories

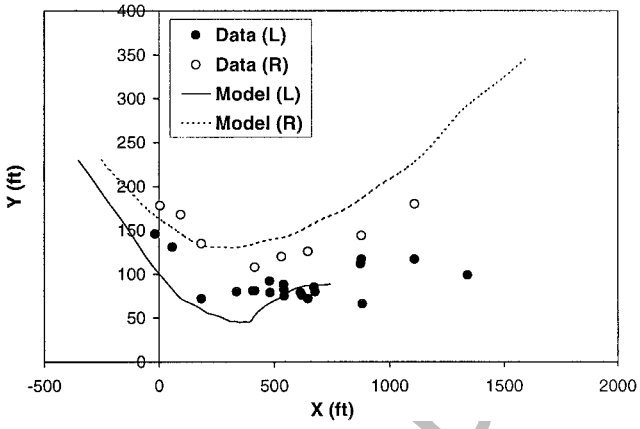

Trajectories

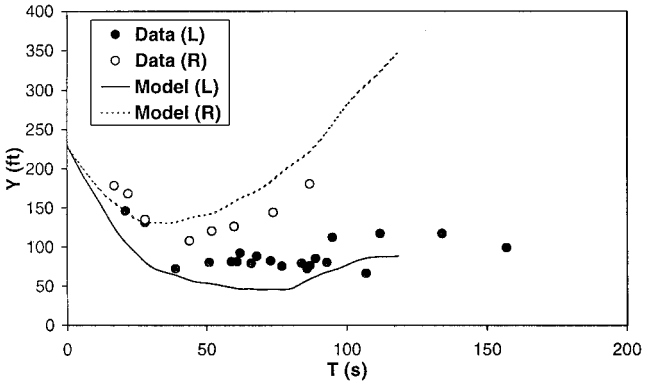

Altitude histories

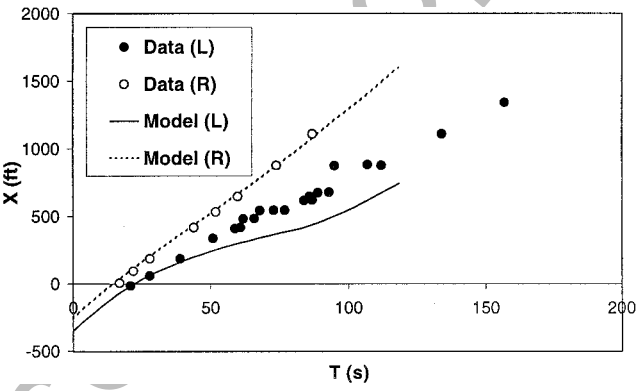

Lateral motion histories

Fig. 5 Comparison of the model results with field-measurement data of the run 9 case.

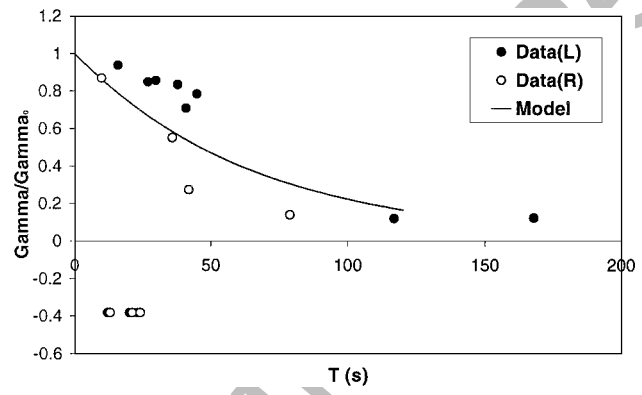

Vortex decay histories

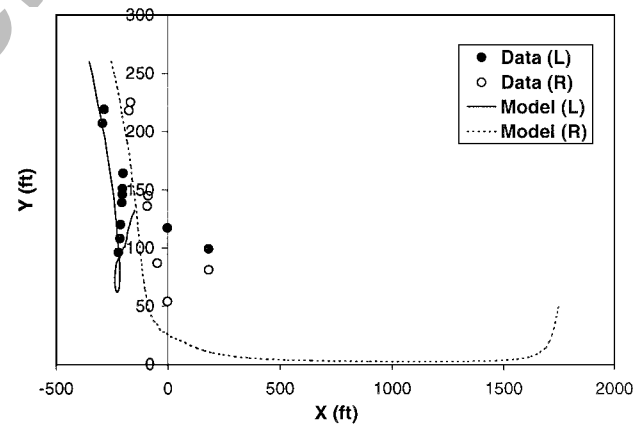

Trajectories

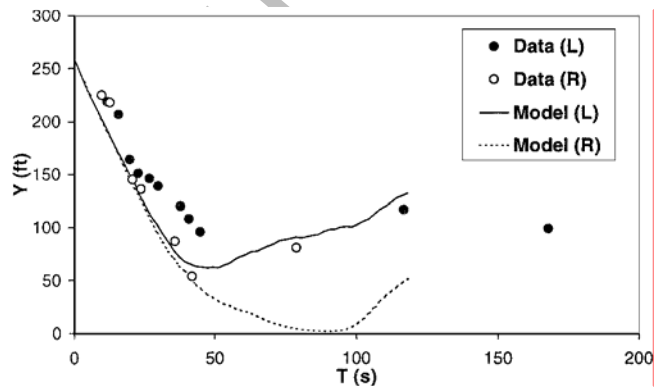

Altitude histories

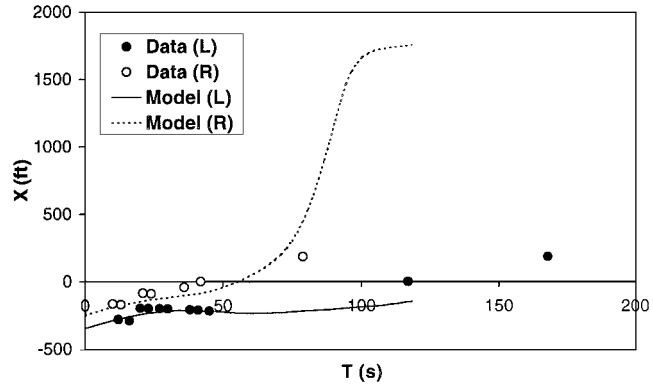

Lateral motion histories

Fig. 6 Comparison of the model results with field-measurement data of the run 45 case.

The purpose is to mimic the effects of atmospheric turbulence on the wake vortex pair, which decays the strength of wake vortices. The circulations of shear vortices remain unchanged.

An automated shear detection algorithm (ASDA) has been developed to read in the wind measurement data and output the shear information as input for the vortex model. The algorithm is explained in the following flow chart: read in meteorological data → cubic spline curve fitting → output results obtained from curve fitting → determine the maximum slope → finding the location of strongest shear → using the least-squares interpolation to determine the shear-layer strength.

Figure 3 is part of the output from ASDA's spline-curve-fitting subroutines. In identifying the shear-layer information for the model input, the algorithm performs best when the strength and location of a strong, concentrated shear can be clearly determined. The shear-layer properties as output of ASDA for the three test cases have been listed in Table 1. Each procedure in ASDA is coded with a subroutine of FORTRAN 90 programs. The cubic splines and least-squares interpolations call the subroutines in the International Mathematics and Statistics Library. To verify the performance of ASDA, the parameters output by ASDA were compared with those determined on the basis of the case-by-case hand calculations and showed very close agreement.

In Table 1, the shear properties in the model are related as

$$(u_1 - u_2)/2 = (H/\Delta y + 1)(\Gamma_s/2\Delta x) \tag{3}$$

where u_1 and u_2 are the wind velocities at the top and bottom of the shear layer, respectively; H is the thickness of the shear layer; Γ_s is the circulation of the vortices in the shear layer used in the model; and Δx and Δy are the lateral and vertical spacing of the shear layer vortices, respectively. The simulation results should be independent of the shear-layer vortex spacing, Δx and Δy, if they are properly chosen. The values of Δx and Δy are determined when sensitivity tests provide reasonable grid-spacing independent results.

The shear strength in each case is determined as $(u_1 - u_2)/H$, and the shear thickness, H, represents the broadness of the shear layer. In run 22, the shear strength is 0.082/s within a narrow altitude range of 14.2 m. The shear strength and thickness in run 9 are 0.0634/s and 68 m, respectively. The shear is still strong in this case but is not concentrated. In run 45, the shear strength is 0.037/s and is distributed in a broad range of 122 m. It should be pointed out that Γ_s itself is not indicative of shear strength.

Figures 4–6 are the comparisons among the measured and calculated circulation decay, vortex trajectories, and altitude and lateral position histories for both the right and left vortices in the wake vortex pair for the three cases. Figure 4 shows that in run 22, the model predicts the deflection of the right vortex very well, which is caused by a strong shear below the wake vortex pair. Rebound of the left vortex is underpredicted, possibly because it is closer to the ground and viscous ground effects[8] might play a role. Figure 5 is run 9 and still shows reasonable agreement between the model and the measured data, although the shear is slightly broader in this case. The overprediction of the right vortex deflection can be attributed to the same reason as stated: the excluded decay of shear-layer vortices in the model. It has been noted in Ref. 4 that the shear/vortex interaction model performs best when there is a concentrated, strong shear, which is the case in run 22. Therefore, in the case of a weak, broad shear, as in run 45, Fig. 6 shows discrepancies in trajectory histories between the model data and the measurement. In this case, the shear layer is spread between 24 and 146 m from the ground. According to Table 1, the shear is located both above and below the wake vortex pair. The right vortex, which has the opposite-sign vorticity of the shear, approaches very close to the ground, and the viscous effects of the ground should be more important than the shear effects. The excessive lateral motion of the right vortex in the model results is also caused by the closeness of the right vortex to the ground, which produces strong interactions between the right vortex and its image vortex at the negative side of the ground boundary. However, the predictions of the left-vortex trajectory seem reasonable, because now the left vortex is farther away from the ground than the right vortex.

Shear Thickness Effects and Wind Measurement Requirement for the Model Input

In Eq. (3), the shear thickness H is related with the resolution of wind measurement from the NASA AVOSS operation point of view. According to the meteorological profile in the AVOSS wind analysis system developed by MIT Lincoln Laboratory,[11] it now has a 15-m resolution from 15 to 150 m and a 50-m resolution from 200 to 1400 m. We have conducted model simulations to determine the resolution requirement for the input in our model for the shear strength based on Eq. (3). The purpose is to test the sensitivity of the trajectory prediction against the resolution of the wind profile measurement. Figure 7 illustrates the resolution issue in the measurement: what happens if the same wind profile, quantified by u_1 and u_2, is measured with resolution of H_2, which is different from the real shear thickness H_1?

Figure 8 shows sensitivity tests when the shear thickness is half of the initial vortex-pair spacing ($0.5B_o$, where $B_o = 25$ m), compared with the shear having the same measured wind speed but a more

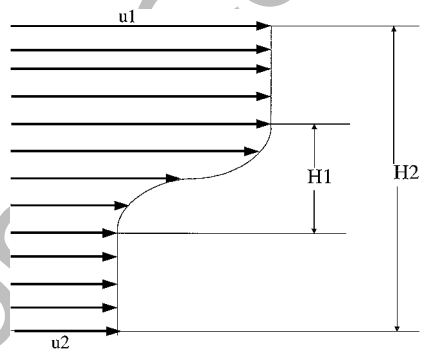

Fig. 7 Windshear profile and measured quantities.

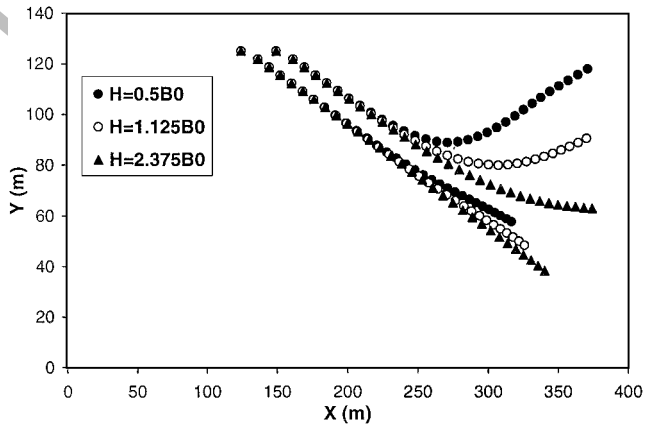

3 m/s shear case

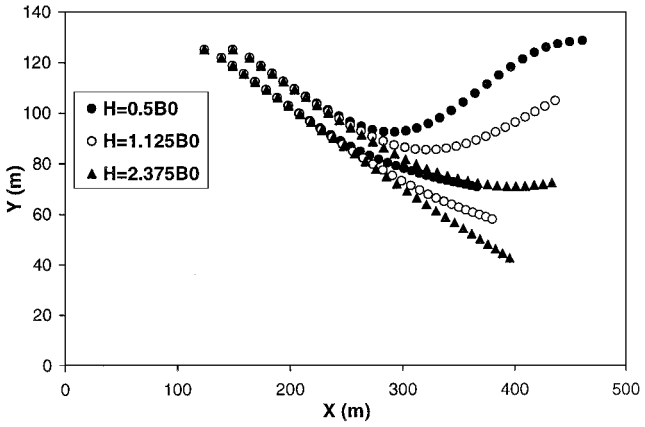

4 m/s shear case

Fig. 8 Sensitivity tests of shear thickness.

coarsely resolved thickness. The concentrated shear cases with 3 and 4 m/s wind speed change, the same as those in Fig. 2, were selected for testing. In each case, the numerical resolution, Δx and Δy (with values of $0.5B_o$ and $0.125B_o$, respectively), remains the same. The circulation of the shear vortices changes correspondingly due to the shear thickness change. It can be seen that the two results for the shear thickness of $0.5B_o$ and $1.125B_o$ are within the accuracy range that a field measurement can reach. The vortex deflection is captured in both the 3 and 4 m/s shear cases. If the wake-generating aircraft is a Boeing 757-200 and its wake vortex pair initial spacing is 30 m, the wind measurement resolution for shear thickness can be as coarse as 30 m, although the real shear thickness is only 15 m. Of course, this is assuming that there is only one strong shear layer ($\partial u/\partial y = \text{const}$) within the 30-m range. In fact, none of the wind profiles in the IDF measurement[5] showed more than one strong shear layer within 30 m. Figure 8 also shows that if the resolution is more than four times the real shear thickness, the errors become large.

Conclusion

The wake vortex/shear interaction model has been validated by using both N–S simulations with large-eddy turbulence models and the field measurement data. It has been shown that when the vortex is not very close to the ground boundary and there exists a strong shear layer in the atmosphere, the model predictions have good agreement with the measurement data. The model can accommodate the wind profile resolution from meteorological measurement. A sensitivity test shows that with a concentrated shear, vortex deflection can still be simulated within reasonable accuracy when the wind measurement resolution is two times coarser than the shear-layer thickness. For a wake-generating aircraft the size of a Boeing 757-200, the wind measurement resolution can be as coarse as 30 m. An automated shear detection algorithm used to preprocess the meteorological wind measurement for the model input has been developed and tested. Implementation of the model for real-time prediction is feasible because of the reduced computer time compared with N–S simulations and the proper flow physics included to predict the asymmetric deflection of the wake vortices.

Acknowledgments

This research was partly under the support of NASA Research Grant NAG1-1911 from the NASA Langley Research Center. The authors would like to express their deep appreciation to F. H. Proctor at the NASA Langley Research Center for providing the large-eddy simulation data and detailed comments on the draft of this paper.

References

[1]Proctor, F. H., Hinton, D. A., Han, J., Schowalter, D. G., and Lin, Y. L., "Two Dimensional Wake Vortex Simulations in the Atmosphere: Preliminary Sensitivity Studies," AIAA Paper 97-0056, Jan. 1997.

[2]Hinton, D. A., "An Aircraft Vortex Spacing System (AVOSS) for Dynamic Wake Vortex Spacing Criteria," *AGARD 78th Fluid Dynamics Panel Meeting and Symposium*, Paper 23, Trondheim, Norway, May 1996.

[3]Mathews, M. P., Dasey, T. J., Perras, G. H., and Campbell, S. D., "Planetary Boundary Layer Measurements for the Understanding of Aircraft Wake Vortex Behavior," American Meteorology Society, Paper 5-5, Long Beach, CA, Feb. 1997.

[4]Zheng, Z. C., and Baek, K., "Inviscid Interactions Between Wake Vortices and Shear Layers," *Journal of Aircraft*, Vol. 36, No. 2, 1999, pp. 477–480.

[5]Garodz, L. J., and Clawson, K. L., "Vortex Wake Characteristics of B757-200 and B767-200 Aircraft Using the Tower Fly-By Techniques," Environmental Research Lab., Air Resources Lab. Rept. 199, National Oceanic and Atmospheric Administration, Idaho Falls, ID, Jan. 1993.

[6]Corjon, A., Zheng, Z. C., and Greene, G. C., "Model of the Behavior of Aircraft Wake Vortices Experiencing Crosswind Near the Ground," AIAA Paper 96-2516, June 1996.

[7]Ash, R. L., and Zheng, Z. C., "Numerical Simulations of Commercial Aircraft Wakes Subjected to Airport Surface Weather Conditions," *Journal of Aircraft*, Vol. 35, No. 1, 1998, pp. 18–26.

[8]Zheng, Z. C., and Ash, R. L., "A Study of Aircraft Wake Vortex Behavior Near the Ground," *AIAA Journal*, Vol. 34, No. 3, 1996, pp. 580–589.

[9]Greene, G. C., "An Approximate Model of Vortex Decay in the Atmosphere," *Journal of Aircraft*, Vol. 23, No. 7, 1986, pp. 566–573.

[10]Sarpkaya, T., "A New Model for Vortex Decay in the Atmosphere," AIAA Paper 99-0761, Jan. 1999.

[11]MIT Lincoln Lab. Wake Vortex Program Monthly Technical Letter, May 1998, 43-MLR-WV [98-02/3/4].